Author's Accepted Manuscript

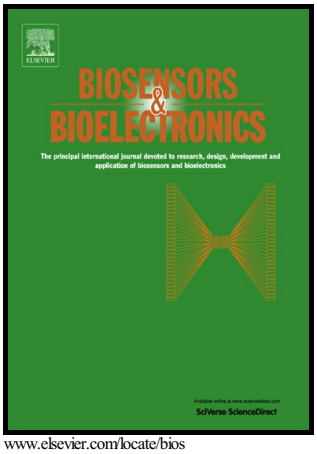

www.elsevier.com/locate/bios

A novel electrochemical biosensor for antioxidant evaluation of phloretin based on cell-alginate/L-cysteine/gold nanoparticle-modified glassy carbon electrode

Yongli Ye, Jian Ji, Fuwei Pi, Huicheng Yang, Jie Liu, Yinzhi Zhang, Shuang Xia, Jiasheng Wang, Dan Xu, Xiulan Sun

PII: S0956-5663(18)30554-2
DOI: https://doi.org/10.1016/j.bios.2018.07.051
Reference: BIOS10640

To appear in: *Biosensors and Bioelectronic*

Received date: 29 May 2018
Revised date: 19 July 2018
Accepted date: 25 July 2018

Cite this article as: Yongli Ye, Jian Ji, Fuwei Pi, Huicheng Yang, Jie Liu, Yinzhi Zhang, Shuang Xia, Jiasheng Wang, Dan Xu and Xiulan Sun, A novel electrochemical biosensor for antioxidant evaluation of phloretin based on cell-alginate/L-cysteine/gold nanoparticle-modified glassy carbon electrode, *Biosensors and Bioelectronic,* https://doi.org/10.1016/j.bios.2018.07.051

A novel electrochemical biosensor for antioxidant evaluation of phloretin based on cell-alginate/L-cysteine/gold nanoparticle-modified glassy carbon electrode

Yongli Ye[a], Jian Ji[a], Fuwei Pi[a], Huicheng Yang[b], Jie Liu[a], Yinzhi Zhang[a], Shuang Xia[a], Jiasheng Wang[a], Dan Xu[c], Xiulan Sun[a,*]

[a]School of Food Science, State Key Laboratory of Food Science and Technology, National Engineering Research Center for Functional Food, School of Food Science Synergetic Innovation Center of Food Safety and Nutrition, Jiangnan University, Wuxi, Jiangsu 214122, PR China

[b]Guangzhou GRE Metrology & Test Co., Ltd, Guangzhou, Guangdong, 510000, PR China

[c]School of Food and Biological Engineering, Shaanxi University of Science and Technology, Xi'an 710021, PR China

*Corresponding author: Xiulan Sun (E-mail: sxlzzz@jiangnan.edu.cn)

ABSTRACT

Antioxidant evaluation of bioactive compounds is limited, since many methods lack a real physiological environment that can be used conveniently and intuitively. In this study, a simple, label-free and effective electrochemical biosensor method has been developed to evaluate the antioxidant effect of phloretin (Ph) by 3D cell modification on a glassy carbon electrode (GCE). In response to this, A549 cells were immobilized onto a self-assembled L-cysteine/gold nanoparticle (AuNPs/L-Cys)-modified GCE surface by a simple drop casting after encapsulated in alginate. The electrochemical impedance spectroscopy (EIS) results showed that the impedance value (R_{et}) increased with the concentration of H_2O_2 in the range of 0-60 μmol/L with the correlation of 0.990 which acted as an oxidative stress model inducer. However, the EIS value decreased with the co-incubation of Ph ranging from 10 to 100 μmol/L, showing a dose-dependent manner and time effect, indicating that the

variation of R_{et} was responded to the antioxidant effect. The response impedance of the biosensor is linear to Ph concentrations from 20 μmol/L to 100 μmol/L with the detection limit (LOD) as 1.96 μmol/L. A significant correlation was observed between reactive oxygen species (ROS) values and R_{et} values following the concentrations of Ph, thus demonstrating the good biological relevance of cell-based electrochemical method. The strategy has been used to evaluate Ph antioxidant capacity in real cells with satisfactory results, indicating the feasibility of biosensor analysis for antioxidant evaluation.

Keywords

Electrochemical biosensor, Antioxidant, Electrochemical impedance spectroscopy (EIS), Phloretin, A549 cell

1. Introduction

Antioxidants perform various beneficial functions as a defense mechanism against oxidative damage in the living organism. Antioxidant activity of these compounds usually refers to the scavenging ability of free radicals (Brewer, 2011; Halliwell, 2011). Thus, from a nutritional point, it is important to evaluate the antioxidant potential of phytochemicals and food products so as to assess their health benefit. In recent years, considerable attention has been devoted to the influence of free radicals on different constitutions of cells, even animals, and the relationship with antioxidant foods or herbal supplements that are rich in natural antioxidant components, especially fruits and vegetables are ordinarily contained in the human diet (Yang et al., 2017). Various antioxidants, phenolic and flavonoid compounds are well-known for their potential to scavenge free radicals and reactive oxygen species (ROS), and exhibiting numerous health benefits (Zuo et al., 2011; Riebel et al., 2017). In line with this hypothesis is the widely accepted view that the positive health effects of active factors can be attributed to their antioxidant activity. Phloretin (Ph) is a dihydrochalcone that belongs to the flavonoid family of polyphenols and high levels are present in the peel and root skin of frequently consumed fruits and vegetables (Rezk et al., 2002; Crespy et al., 2002; Wei et al., 2017). A great amount of evidence

demonstrates that Ph can exert wide biological and pharmacological activities, including antioxidant, anti-inflammatory, anti-cancer , and other beneficial effects to human health (Liu et al., 2015; Barreca et al., 2014; Lin et al., 2016). Especially its antioxidant properties, has been caused an increasing interest. However, the lack of rapid antioxidant evaluation tools based on the changes in physiology and biochemistry of organism makes the development of a simple, rapid, and sensitive approach for antioxidant evaluation of Ph necessary.

Currently, there are four general types of assays that are used for the evaluation of antioxidant activity, including chemical assays (Lim et al., 2007), instrumental assays (Tang et al., 2008; Qiu et al., 2012; Riethmuller et al., 2015), cell-based assays (Wan et al., 2015) and animal model / human assays (Niki, 2010; Liu et al., 2015). Owing to the advantages of low cost, convenience, sensitivity and rapid operation, chemical assays are widely used to evaluate antioxidant of interest in food and health, disease and therapy (Dai et al., 2013; Geng et al., 2015; Zhang et al., 2017). However, for the reason of complex substrates, compositions as well as analytical methods (both of the chemical assay and instrumental assay are performed in test tubes under non-physiological conditions), it remains questionable whether the results can be used to predict the antioxidant capacity *in vivo*, and they cannot imitate the internal physiological environment of the organism (Zhu et al., 2017; Frankel and Meyer, 2000). Although animal model/human assay can truly reflect the antioxidant effect *in vivo*, the significant expense and time consumption render this assay unsuitable for the antioxidant evaluation in the initial stage of research in the food field. The cell is the basic site of oxidative stress reaction and the antioxidant capacity which is expressed in cell level can promote more biological significance. In this case, a cell-based assay is an attractive, promising and feasible method.

In contrast, the application of electrochemical sensors for the evaluation of antioxidants has gained attention for its rapid response, high sensitivity and ease of miniaturization (Fu al., 2018; Ni al., 2018; Barroso al., 2015). As one of the most enduring biosensors, cell-based electrochemical biosensor can detect biochemical effects directly via living cells with unique advantages of noninvasiveness, label-free

experimentation, fast response time, high efficiency and versatile fabrication (Jeonget al., 2012). This method can even mimic *in vivo* cellular conditions by supporting cell growth and maintaining morphogenesis, cell metabolism and cell-to-cell interactions normalization by employing a three-dimensional (3D) scaffold. This biosensor can also convert the effects into digital electrical signals compared with the traditional antioxidant detection technique by sensors and transducers (Liu et al., 2014). In general, the electrochemical technique serves as a bridge between biology and electronics, and provides a powerful tool to study the physiological effects of analytes on cells (Ding et al., 2007).

In this study, a novel cell-based electrochemical biosensor was developed for an oxidative damage model and the antioxidant evaluation of Ph on a 3D cell culture. Metal nanoparticles, such as gold nanoparticles (AuNPs), cobalt oxide nanoparticles, have the unique advantages of high conductivity, biological compatibility, chemical stability, and electrocatalytic properties which cause acceleration of electron transfer rate (Roushani & Sarabaegi, 2014; Roushani & Shahdost-fard, 2015; Ghanbari, 2018). Furthermore, L-cysteine (L-Cys) can provide abundant active sites for binding analytes and tunable conductivity as an electrochemical sensor material (Arvand et al., 2018; Johnson and Holcombe, 2005). Therefore, we combined AuNPs with L-Cys used to immobilize alginate-cells mixture to fabricate a cell electrochemical sensor. Subsequently, both the cell concentration and treatment conditions were optimized and evaluated. Different electrochemical responses caused by the oxidative damage and protection of antioxidant on A549 cells were recorded. The results showed a good correlations between the antioxidant concentration and the EIS signal. In addition, the verification test results showed that our 3D-cell-based biosensor evaluation can be an alternative method for antioxidant activity evaluation of functional factors.

2. Materials and Methods

2.1. Materials and apparatus

L-cysteine, chloroauric acid ($HAuCl_4 \cdot 4\ H_2O$) and alginate from brown algae (low viscosity) were obtained from Sigma-Aldrich Inc (St. Louis, MO, USA). Phloretin

(molecular weight = 274.27, purity N 98%, verified by high-performance liquid chromatography; provided by Phytomarker, China) was dissolved in dimethyl sulfoxide (DMSO) to make a 200 mM stock solution and stored at 4 ℃ for further use. Human lung adenocarcinoma epithelial cells (A549) were obtained from Tongpai Biological Technology Co., Ltd (Shanghai, China). Type I collagen (rat tail, collagen-I) was purchased from BD Biosciences (Alginaten Jose, CA, USA). Dulbecco's minimal essential medium (DMEM) and fetal bovine serum (FBS) were obtained from Gibco Laboratories (Gaithersburg, MD, USA). All solutions were prepared with ultrapure water and all reagents were of analytical grade. Dichloro-dihydro-fluorescein diacetate (DCFH-DA), Lacate dehydrogenase (LDH), and malondialdehyde (MDA) assay kits were purchased from the Beyotime Biotechnology Co., Ltd (Nantong, China).

A549 cells were incubated in a CO_2 incubator (Thermo Scientific Forma Series ⅡWater Jacket, Thermo Fisher Scientific Inc., Rockford, IL, USA). Glassy carbon electrodes (GCEs) of 4 mm^2 and corresponding linking devices were obtained from Shanghai Chenhua Instrument Co., Ltd (Chenhua, Shanghai, China). Electrochemical experiments were performed with the CHI660e electrochemical workstation (Chenhua, Shanghai, China) using a conventional three-electrode system in a solution containing 2.5 mM of $Fe(CN)_6^{3-/4-}$ and 1.0 M KCl. The morphologies of cells mixed with gel on GCE were characterized by scanning electron microscopy (model Hitachi SU8000 and S-4800, Hitachi Co., Ltd., Tokyo, Japan). The CCK-8 assay and ROS assay were measured using a microplate reader (Spectra MAX 340, Molecular Devices Co., Sunny vale, CA, USA). The fluorescence imaging of ROS concentration was detected by a wide field high-content analysis system (Image Xpress Micro XLS, Molecular Devices, USA).

2.2. Cell culture

A549 cells were cultured for continuous logarithmic-phase growth in a medium provided by high-glucose DMEM and 10% fetal bovine serum (FBS, GIBCO, US) in T-150 tissue culture flasks. Cells were incubated at 37 ℃ in 5% CO_2, 95% air humidified atmosphere. Culture medium was maintained fresh by changing every

other day as needed.

2.3. Preparation of AuNPsCys-modified GCE and cell immobilization

Prior to modification, the GCE was polished with 0.3 μm and 0.05 μm alumina slurry on a polishing cloth, followed by successive sonication in ethanol and deionized water for 5 min and then dried under a stream of nitrogen. Before the voltammetric measurement, the bare electrode was cycled between -0.6 and 0.6 V (scan rate, 100 mV/s) several times until reproducible responses were acquired. The GCE stepwise fabrication is shown in Scheme 1. The modification of GCE with AuNPs was achieved by using electrodeposition to deposit AuNPs on the GCE in a 0.5 M H_2SO_4 solution containing 1 mM of $HAuCl_4$, under a constant potential of -0.25 V, for an optimal time of 100 s to improve electron transfer efficiency and then washed in doubly-distilled water (Jiang et al., 2013). The obtained AuNP-modified GCE was immersed in 1mg/mL L-Cys solution for 3 h and then rinsed multiple times with doubly-distilled water to eliminate physically adsorbed L-Cys, and dried with N_2. The resulting AuNPsCys modified electrode was stored at 4 ℃ for further use.

A549 cells were encapsulated in alginate gel for biosensing is described as followed: logarithmic phased grown A549 cells were collected, counted, washed, and resuspended in 10% FBS-supplemented DMEM medium with 3% alginate solution to a final concentration of 1×10^6 cells/mL in 1% alginate solution. Then 10 μL of the alginate-cells mixture was dropped on AuNPsCys modified GCE surface at 37 ℃ in 5% CO_2, 95 % air humidified atmosphere for 3 h to achieve cell immobilization for further electrochemical measurements.

More details regarding the Characterization, Electrochemical experiments and Statistical analysis were shown in Supporting Information (SI).

3. Results and discussion

3.1. Suitability of inducer and antioxidant for use in the sensor system

The capacity to modulate a variety of cell functions, cross membranes, and diffuse away from the site of generation, makes hydrogen peroxide (H_2O_2) an ideal signaling molecule. Therefore, our study used H_2O_2 as the reactive oxidant to

establish a damage model. It should be noted that high levels of H_2O_2 are cytotoxic to a wide range of cells, although the effect depends on multiple parameters such as cell type, iron content, time of exposure to H_2O_2, and the culture media employed. However, many studies reported that Ph can affect the growth of some cancer cells and induce apoptosis (Wu et al, 2017). Thus, we investigated the appropriate concentration range of the inducer and antioxidant initially as the basis of the subsequent electrochemical biosensor test.

With different treatment conditions of H_2O_2, results showed that the cells followed with a decline in viability at higher concentrations and extension time. As shown in Fig. 1 A, when treated for 4 h, at below 80 μmol/L of H_2O_2, the cell viability slightly decreased compared to 2 h ($P>0.05$), but the necrotic condition was significantly lighter than for 6, 8 and 10 h of treatment ($P<0.05$, which compared with the results of 2 h treatment). The doses of H_2O_2 exceeding 80 μmol/L exhibited extremely decrease of cell viability under all treatment times. While a high degree of oxidative stress can cause necrosis, lower levels will trigger apoptosis. Therefore, since free radicals are generated more at higher survival rates of cells, different concentrations (0-80 μmol/L) of H_2O_2 treatment for 4 h for A549 cells were used as the subsequent conditions.

Higher concentrations of Ph also caused apoptosis (Fig. 1 B). While A549 cells treated with Ph of the concentration range from 10-200 μmol/L for 24 h, the viability declined gently, indicating that there was less negative influence of Ph on cells within the short incubate time at this dose range. But for 48 h treatment, there was a 43.44% decrease in the viability of the cells at 100 μmol/L of antioxidant compared to control cells ($P=0.004<0.05$). To maintain the cytoactivity, a Ph concentration between 10 μmol/L and 100 μmol/L was used and the processing time was controlled within 24 h.

3.2 *Characterization of the AuNPsCys-modified GCE*

The entire AuNPs/L-Cys/GCE modification is briefly described in Scheme 1. The GCE was modified with AuNPs to further enhance the GCE sensitivity. Generally, AuNPs were deposited on the surface of a clean bare GCE (deposition time ranging from 0 to 180 s) (as shown in Fig. S 1). Since they are uniformly distributed on the

electrode surface, the AuNPs not only enlarged the surface area but also improved the adsorptive capability of the biomolecules (Roushani & Farokhi, 2016). According to optimization results, when time exceeded 100 s, peak current almost became steady; therefore, we chose 100 s as the deposition time to modify GCE (Fig. 2 A). Subsequently, L-Cys was self-assembled onto the AuNP/GCE via strong coordination interactions of its thiol-groups with nanoparticles (Xia et al., 2017). Finally, the cell-alginate mixture of optimized concentration was dispensed onto the AuNPs/L-Cys-modified GCE.

3.3 Electrochemical characteristics of A549 cells on a modified electrode

The characteristics of the biosensor process and the A549 cells adsorption on modified GCE surface were tested by CV, DPV and EIS. As shown in Fig. 2 B, the voltammograms showed a typical reversible redox peak at the bare GCE surface (curve a), then the current increased significantly when the bare electrode was modified with AuNPs (curve b), due to its excellent conductivity as well as the increased effective area of the electrode. The L-Cys containing a thiol residue on the terminus were then self-assembled on the AuNP/GCE via an Au-S covalent bond, and the amino group on the other terminus was used to react with cells and alginate gel to make a more stable adhesion. L-Cys modification on the working electrode caused the current decrease, reflecting that the L-Cys layer was successfully assembled on the AuNPs/GCE surface (curve c). When the alginate-cells mixture was immobilized onto the electrode surface, a strong decrease peak current was observed (curve e). This result may be caused by an electron transfer blockage in the mixture which increased the electrode resistance increased (Jiang et al, 2013). The similar signal changes of DPV results and the opposite signal changes of EIS results are shown in Fig. S 2.

The EIS of the modified electrode showed that the electron transfer resistance (R_{et}) increased following by self-assembly (Fig. S 2 B). With bare GCE, the resistance was 357.40 ± 27.42 Ω, when AuNPs were assembled on the bare electrode, a dramatically low R_{et} of about 33.99 ± 7.37 Ω was obtained (SEM images of both bare GCE and AuNPs/GCE are shown in Fig. S 3). This result was consistent with the views illustrated above, suggesting the nanoparticle layer can increase the interfacial

electron transfer. For the reason of the insulating properties of L-Cys, the R_{et} was increased to 202 ± 20.20 Ω and continued to increase after deposition of the alginate-cells mixture on the modified electrode until the value reached 1042.12 ± 26.63 Ω. The concentrations of A549 cells, ranging from 1×10^3 to 1×10^7 cells/mL, encapsulated in alginate were optimized (Nyquist diagrams are shown in Fig. 2 C). The increasing diameter of the semicircle showed that the R_{et} increased follow by increasing cell concentration, linear regression equations was y = 246.4x + 55.767 (x was the log transformed A549 cells number) with a good correlation coefficient (R^2) of 0.998. This suggests that a higher number of cells were successfully immobilized on the electrode. Considering the negative effect of high cell density on the precision of the result, 1×10^6 cells/mL was chosen as appropriate attached cell number for antioxidant evaluation according to the result of R_{et} measurement.

In previous studies, we constructed a 3D cell culture model on the electrode effectively by using collagen. Thus, we proposed to use alginate as the 3D stand material, and the collagen as the control treatment to evaluate the effectiveness of the model we had established. The impedance of which A549 cells encapsulated in alginate was 1135 ± 50.98 Ω; however, instead, Type I collagen increased the R_{et} extremely for its compactness (5830 ± 75.06 Ω). Moreover, the collagen was coagulated easily which made it hard to operate. The Nyquist diagrams and SEM images results (Figs. 2 D, 2 E) suggest that alginate can supply A549 cells nutrition and maintain cells viability.

3.4 A549 cell biosensor evaluated the H_2O_2 damage

H_2O_2-mediated A549 cells oxidative damage leads to the initiation of a signaling cascade, resulting in the release of related proteins. Thus, we expected to monitor and determine the cell-electrode impedance response of cells under oxidative stress conditions by variating cell morphology and metabolism. In this process, H_2O_2-induced cells caused oxidative stress and the parameters used were based on the previous experimental results as a model to illustrate the R_{et} variation of oxidative damage. EIS from A549 cells was induced by a variety of concentrations of H_2O_2, and showed a dose-dependent relationship (Fig. 3 A). When the additive ranged from 0 to

60 μmol/L, it was showed that the semicircle diameter was increased in the Nyquist diagram, and the R_{et} value was proportional to the utilized H_2O_2 concentrations, with a linear equation of y (Ω) =19.4C_{H2O2} + 1641.1 (R^2 = 0.990). However, the R_{et} value decreased with higher inducer concentrations. At low concentration, the H_2O_2 stimulated cells secreted abnormally, the R_{et} might be increased by the release of various factors from the cytoplasm to the extracellular and other physiological changes. However, high concentrations (> 60 μmol/L) of H_2O_2 induced cell apoptosis and severe cytolysis that made a reduction of the adhesion area on the electrode, and ultimately decreased the R_{et}. This result about the dose-response relationship obtained from electrochemical biosensor measurement agreed well with previous data (Figs. 3 B and 3 C). Thus, the concentration of 60 μmol/L was selected to establish the oxidative stress model on a modified electrode.

3.5 Antioxidant evaluation of Ph by A549 cell biosensor

In the presence of oxidative stress, A549 cells activation led to the initiation of a signaling cascade resulting in the increase of extracellular secretions, which contained protease and related mediators of oxidation reaction such as lactate dehydrogenase (LDH) and thioredoxin (Trx). Considering that the electron-transfer resistance was responded to the cell morphology and metabolism, we attempted to confirm the relationship between antioxidant effect and field impedance. Consequently, cells were co-stimulated with various concentrations of Ph and a specific inductive dose of H_2O_2 under different treatment times.

According to the impedance values of A549 cells in our experiments, as Ph concentrations increased from 10 to 100 μmol/L, the EIS variation rate of A549 cells significantly decreased at different treatment times (as shown in Fig 4). EIS results from A549 cells treatment groups showed a dose-dependent relationship in response to treatment for 2, 4, 6 and 8 h, respectively (Fig. S 4). The most important factor that contributed to the successful recording of a change in the impedance was a high exocytosis expression. With prolonged treatment time and increased Ph concentration, the diameter of the semicircle was gradually decreased during testing, indicating that the EIS variation rate decreased, and that the antioxidant effect was valid. When cells

were co-incubated for each experiment time point, the rates of treatment doses above 20 μmol/L were significantly decreased compared to the induced oxidative damage group. The lowest impedance values were obtained while the concentrations of Ph was 100 μmol/L at all treatment times (the oxidant damage rates were 182.78 ± 9.52%, 150.25 ± 8.37%, 146.32 ± 6.22% and 141.25 ± 4.79% for 2, 4, 6 and 8h respectively). These results indicated that a lower R_{et} value and ROS generation rate were obtained by the higher treatment concentration of Ph, and the electrochemical impedance signals were negatively correlated with the antioxidant effect.

3.6 Stability, reproducibility and feasibility of established cell biosensor

To determine whether the result of electrochemical impedance was reliable and promising, a traditional ROS assay was performed to assess antioxidant capacity in comparison to the electrochemical method results. The R_{et} values were converted into the ratio before comparison to the ROS assay results (Fig. 4). We found that EIS was more sensitive at low concentrations compared to the ROS assay. There were no significant differences between the EIS assay and ROS assay results by T-test analysis ($P>0.05$), which indicated that the variation tendency of different treatment times using the proposed electrochemical method was consistent with the results obtained via ROS assay as a whole. Fluorescence detection also yielded the similar effects. As the end product of oxidant stress, LDH and MDA were detected to verify whether the impedance changes are associated with intracellular related factors release. The results of LDH leakage and MDA release after treatment with different Ph dosages are shown in Fig. S5 A. For the 8 h of protective tests (40-100 μmol/L), LDH leakage significantly decreased compared to the positive group ($P<0.05$), the lowest level of LDH leakage was recorded for treatment at 100 μmol/L (17.64±0.94 %) ($P<0.001$). In addition, the levels of MDA release also markedly decreased followed by the increased treatment concentration of Ph ($P<0.05$ for 20 μmol/L treatment compared with positive group), and the lowest MDA content was obtained for treatment at 100 μmol/L (134.22±14.63%) which declined about 2.6-fold compared to the positive group ($P<0.001$). These results illustrate that the antioxidant efficiency of Ph treatment caused a decreased LDH leakage and inhibited lipid peroxidation, which

was consistent with the variation tendency of the EIS results.

As shown in Fig. S5 B, the antioxidant effects of both EIS assay and ROS assay were increased in a range from 20 to 100 μmol/L for 8 h treatment. This indicates a good linear relationship between Ph antioxidant and biosensor detection with R^2 was 0.994 (0.903 for ROS assay, RSD < 5% in every point of concentration, Fig. S5 B), and also a detection limit (LOD) of 1.96 μmol/L of Ph (based on signal/noise (S/N) = 3). In particularly, the electrochemical antioxidant evaluation results were higher than the results of the ROS assay, which might be attributed to the different culture conditions, assay procedures and detection objects. Furthermore, three replicative measurements of five Ph doses by 9 modified electrodes randomly yielded a reproducible signal with the coefficient variation range from 2.69% to 4.86% as outlined in Table S1, showing the modified electrode has a good surface reproducibility.

To evaluate the long-term stability effect, the modified electrodes were stored in refrigerator at -80 ℃ for 10 days (the preservation and resuscitation refer to the usual cell treatment method). Results showed that the impedance of the modified electrode changed slightly and the obtained R_{et} value of the biosensor retained 85 ± 4.52 % of the initial response (data not shown). This test proved that the modified electrode surface is stable and nontoxic to cell during this process. All the results imply that the feasibility of our biosensor could be accepted as a simple and convenient way to evaluate antioxidant in cell level via EIS compared to other antioxidant evaluation methods (Table S2).

4. Conclusion

In this study, we developed a novel protocol for durable, simple and label-free *in vitro* real-time determination of antioxidant based on the direct electron transfer of the oxidative stress reaction. We optimized the modified condition of the electrode and the immobilized quantity of A549 cancer cells to enhance signal effectiveness and verified the reproducibility of electrical measurement for long-term monitoring by an electrochemical biosensor applying 3D cell culture. Living A549 cells were

immobilized on AuNPsCys-fabricated GCE for the antioxidant evaluation. AuNPsCys nanocomposites exhibited excellent electrochemical activity. Alginate film with relatively long stability and biocompatibility provides a platform to adhere living A549 cells directly onto the film surface. In addition, we confirmed the feasibility of the application of the cell-based biosensor for analysis of 3D cell culture to investigate the antioxidant efficacy of Ph. Results showed that the method was successfully applied for evaluating both concentration (range of 10-100 μmol/L) of Ph and treatment time (range of 2-8 h) for antioxidant. The detection signal intensity of R_{et} decreased with the increase of the Ph concentrations, which was consistent with the results of ROS, LDH and MDA assays. The RSD of R_{et} detection results was below 5%, and the LOD was estimated at 1.96 μmol/L of Ph, indicating that investigation provides a methodology for the evaluation of antioxidant, which is highly accurate, simple and time saving. Further research is necessary to verify this conclusion trend such as the mechanism of oxidative stress and the antioxidant protection in A549 cells. Our study is the first to present a novel electrochemical method for designing a 3D cell-based impedance sensor for the evaluation the antioxidant of Ph.

Acknowledgements

This work has been supported by the Postgraduate Research & Practice Innovation Program of Jiangsu Provence (KTCX17_1415), National First-class Discipline Program of Food Science and Technology, Collaborative Innovation Center for Food Safety and Quality Control, National Research Program of China (No. 2017YFF0211303, No. 170768), and the Agricultural Science and Technology Innovation Projectin Shaanxi Province (2015NY002).

References

Arvand, M., Sanayeei, M., Hemmati, S., 2018. Biosens. Bioelectron. 102, 70-79.

Barreca, D., Bellocco, E., Lagana, G., Ginestra, G., Bisignano, C., 2014. Food Chem. 160, 292-297.

Barroso, M.F., Ramalhosa, M.J., Alves, R.C., Dias, A., Soares, C., Oliva-Teles, M.T., Delerue-Matos, C., 2015. Food Control 68, 153-161.

Brewer, M.S., 2011. Compr. Rev. Food Sci. F. 10, 221-247.

Crespy, V., Aprikian, O., Morand, C., Besson, C., Manach, C., Demigné, C., Rémésy, C., 2002. J. Nutr. 131, 3227-3230.

Dai, X., Huang, Q., Zhou, B., Gong, Z., Liu, Z., Shi, S., 2013. Food Chem. 139, 563-570.

Ding, L., Du, D., Wu, J., Ju, H., 2007. Electrochem. Commun. 9, 953-958.

Frankel, E.N., Mayer, A.S., 2000. J. Sci. Food Agr. 80, 1925-1941.

Fu, L., Wang, A., Lyv, F., Lai, F., Zhang, H., Yu, J., Lin, C., Yu, A., Su, W., 2018. Bioelectrochem. 121, 7-10.

Geng, D., Chi, X., Dong, Q., Hu, F., 2015. Ind. Crops Prod. 67, 492-497.

Halliwell, B., 2011. Trends Pharmacol. Sci. 32, 125-130.

Ghanbari, K., Roushani, M., 2018. Bioelectrochem. 120, 43-48.

Jeong, S.h., Lee, D.W., Kim, S., Kim, J., Ku, B., 2012. Biosens. Bioelectron. 35, 128-133.

Jiang, D., Ji, J., An, L., Sun, X., Zhang, Y., Zhang, G., Tang, L., 2013. Biosens. Bioelectron. 50, 150-156.

Johnson, A.M., Holcombe, J.A., 2005. Anal. Chem. 77, 30-35.

Lin, S.T., Tu, S.H., Yang, P.S., Hsu, S.P., Lee, W.H., Ho, C.T., Wu, C.H., Lai, Y.H., Chen, M.Y., Chen, L.C., 2016. J. Agric. Food Chem. 64, 6826-6837.

Lim, Y.Y., Lim, T. T., Tee, J. J., 2007. Food Chem. 103, 1003-1008.

Liu, Q., Wu, C., Cai, H., Hu, N., Zhou, J., Wang, P., 2014. Chem. Rev. 114, 6423-6461.

Liu, Y., Zhang, L., Liang, J., 2015. J. Neurol. Sci. 351, 88-92.

Ni, S., Han, F., Wang, W., Han, D., Bao, Y., Han, D., Wang, H., Niu, L., 2018. Sensor. Actuat. B: Chem. 259, 963-971.

Niki, E., 2010. Free Radic. Biol. Med. 49, 503-515.

Qiu, J., Chen, L., Zhu, Q., Wang, D., Wang, W., Sun, X., Liu, X., Du, F., 2012. Food Chem. 135,

2366-2371.

Rezk, B.M., Haenen, G.R.M.M., Vijgh, W.J.F., Bast, A., 2002. Biochem. Bioph. Res. Co. 295, 9-13.

Riebel, M., Sabel, A., Claus, H., Xia, N., Li, H., König, H., Decker, H., Fronk, P., 2017. Food Chem. 229, 779-789.

Riethmuller, E., Tóth, G., Alberti, Á., Végh, K., Burlini, I., Könczol, Á., Balogh, G.T., Kéry, Á., 2015. J. Pharm. Biomed. Anal. 107, 159-167.

Roushani, M., Sarabaegi, M., 2014. J. Electroanal. Chem. 717-718, 147-152.

Roushani, M., Shahdost-fard, F., 2015. Talanta 144, 510-516.

Roushani, M., Farokhi, S., 2016. Anal. Bioanal. Chem. Res. 3, 101-110.

Tang, D., Li, H.J., Chen, J., Guo, C.W., Li, P., 2008. J. Sep. Sci. 31, 3519-3526.

Wei, Y., Zhang, J., Memon A.H., Liang, H., 2017. J. Mol. Liq. 236, 68-75.

Xia, S., Zhu, P., Pi, F., Zhang, Y., Li, Y., Wang, J., Sun, S., 2017. Biosens. Bioelectron. 97, 345-351.

Yang, H., Xue, X., Li, H., Tay-Chan, S.C., Ong S.P., 2017. Food Chem. 229, 215-222.

Zhang, X., Xu, M., Zhang, J., Wu, L., Liu, J., Si, J., 2017. Ind. Crop. Prod. 102, 164-172.

Zhu, J., Yi, X., Zhang, J., Chen, S., Wu, Y., 2017. J. Chromatogr. B Analyt. Technol. Biomed Life Sci. 1060, 262-271.

Zuo, A., Yu, Y., Li, J., Xu, B., Yu, X., Qiu, Y., Cao, C., 2011. Free Radic. Antioxid. 1, 39-47.

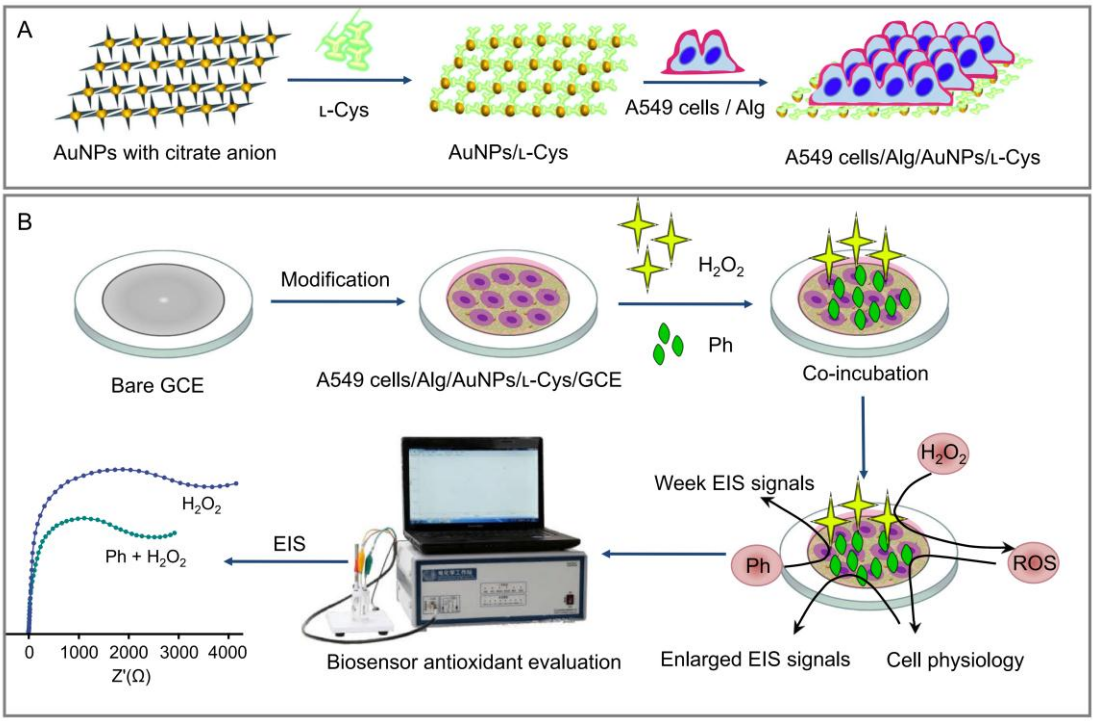

Scheme 1. Schematic illustration for the preparation of A549 cell-based sensor (A) and process of antioxidant evaluation (B).

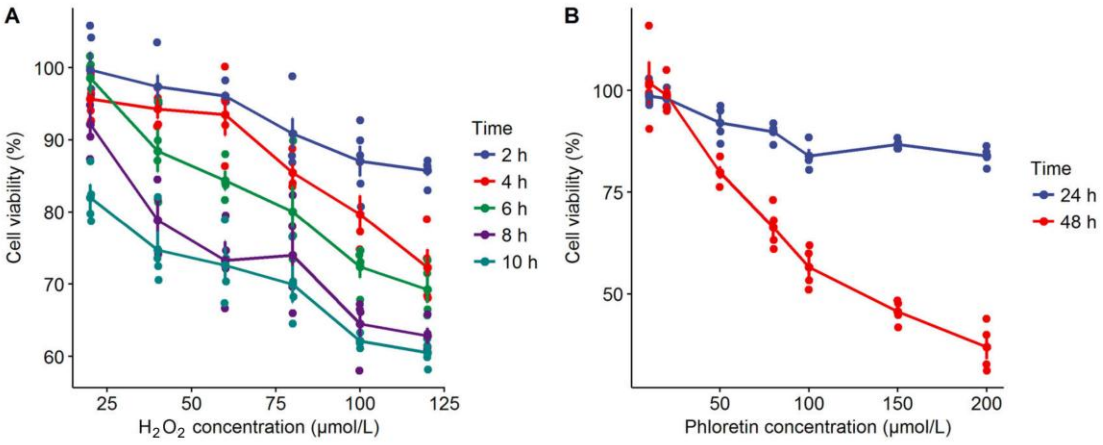

Fig.1. Effects of H_2O_2 and Ph on A549 cells viability. (A) Cell viability for A549 cells treated with different doses (20 to 120 μmol/L) of H_2O_2 for 2 to10 h. (B) Cell viability for A549 cells treated with different doses (10, 20, 50, 80, 100, 150, 200 μmol/L) of Ph for 24 h and 48 h.

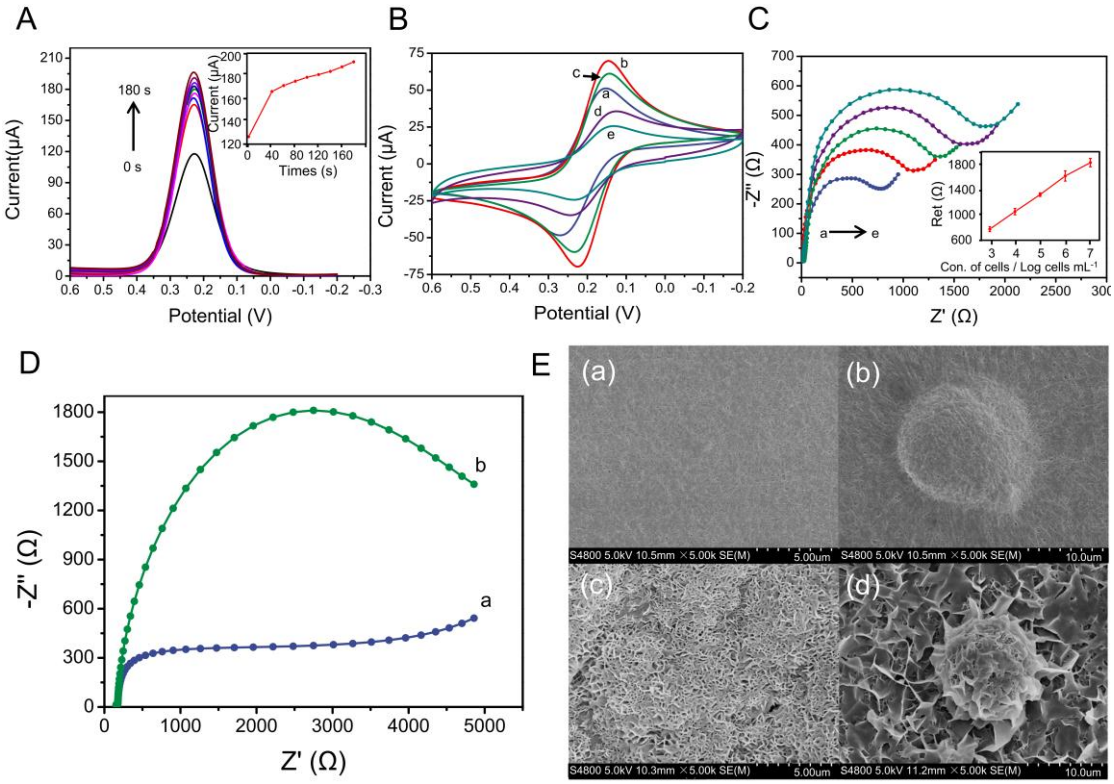

Fig. 2**.** Electrochemical characterization of the modified 3D cell biosensor. (A) DPV of AuNPs modified bare GCE, (B) Voltammograms of (a) bare GCE, (b) AuNP/GCE, (c) L-Cys/AuNP/GCE, (d) alginate/L-Cys/AuNP/GCE, (e) cell/alginate/L-Cys/AuNP/GCE. (C) Nyquist diagrams of 1×10^3 to 1×10^7 cells/mL (a to e) A549 cells immobilized on modified electrode. (D) Nyquist diagrams of (a) cell/alginate/L-Cys/AuNP/GCE, (b) cell/Type I collagen/AuNP/GCE. (E) SEM image of (a) Type I collagen/AuNP/GCE, (b) cell/Type I collagen/AuNP/GCE, (c) alginate/AuNP/GCE, (d) cell/alginate/AuNP/GCE.

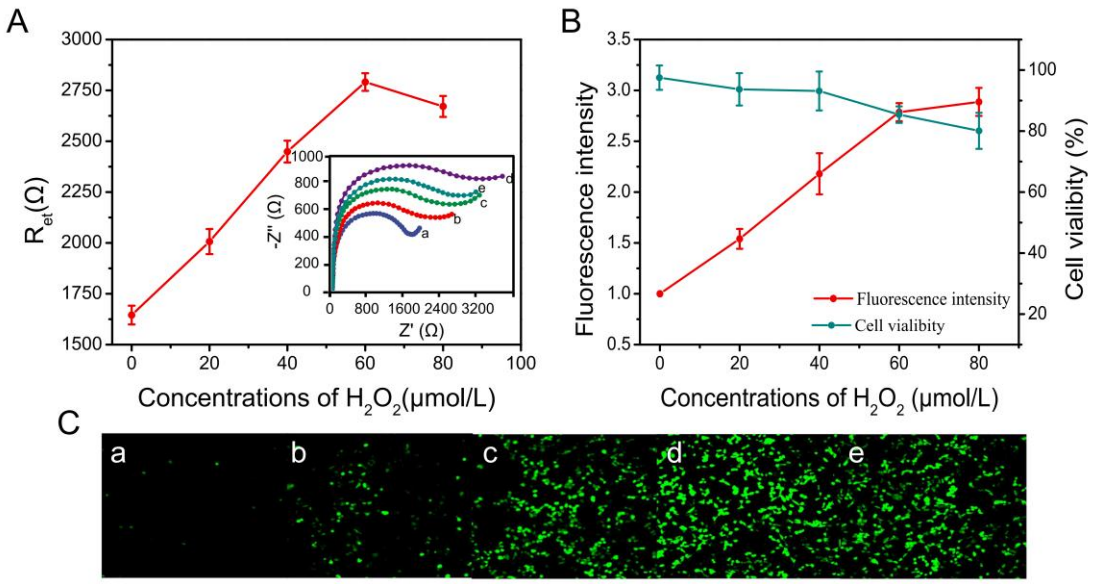

Fig. 3. (A)EIS responses of A549 cells stimulated by H_2O_2. (B) Fluorescence intensity and cell viability obtained by ROS assay. (C) Fluorescent image of ROS in A549 cells with different treatment of (a) 0 to (e) 80 μmol/L of H_2O_2-induced damage.

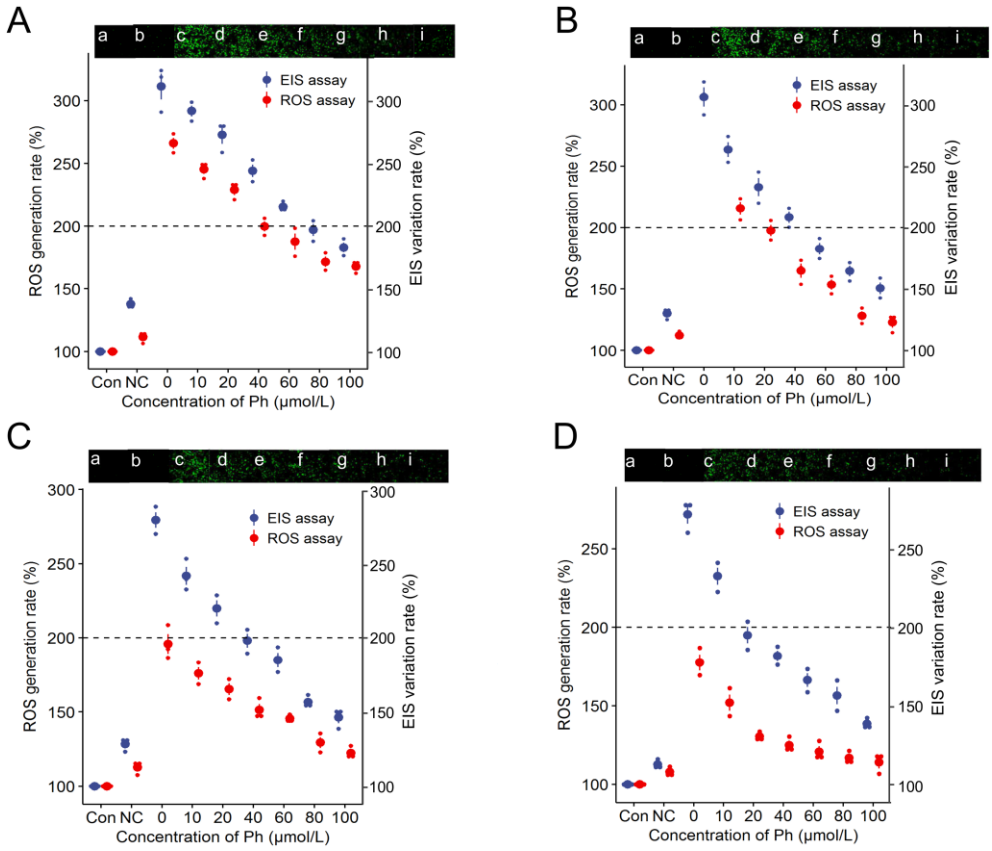

Fig. 4. Antioxidant evaluation effect of Ph in different treatment time by using the proposed

biosensor and ROS assay. The ROS assay results were characterized by ROS generation rate while the EIS assay results were characterized by EIS variation rate. (A) 2 h, (B) 4 h, (C) 6 h, (D) 8 h. Fluorescence images under each scatterplot of (a) to (h): 0 to 100 μmol/L of Ph co-incubation with 60 μmol/L H_2O_2, while Con group was untreated with H_2O_2 and Ph, NC group was only treated with Ph (100 μmol/L).

Hightlights

- A novel cell-based electrochemical biosensor is established to evaluate the antioxidant capacity of phloretin.
- Alginate was used to structure a 3D cell culture to stimulate the in vivo physical environment.
- Electrochemical evaluation of phloretin offers intuitive electrochemical signals and simple antioxidant analysis.
- The developed method can applied as a promising antioxidant evaluation method to other functional factors.